Scripta Materialia 132 (2017) 68–72

Contents lists available at ScienceDirect

Scripta Materialia

journal homepage: www.elsevier.com/locate/scriptamat

Regular Article

Effect of heating rate during primary crystallization on soft magnetic properties of melt-spun Fe-B alloys

B. Zang [a], R. Parsons [a], K. Onodera [b], H. Kishimoto [b], A. Kato [b], A.C.Y. Liu [c,d], K. Suzuki [a,*]

[a] Department of Materials Science and Engineering, Monash University, Clayton, VIC 3800, Australia
[b] Toyota Motor Corporation, Mishuku, Susono, Shizuoka 410-1193, Japan
[c] Monash Centre for Electron Microscopy, Monash University, Clayton, VIC 3800, Australia
[d] School of Physics and Astronomy, Monash University, Clayton, VIC 3800, Australia

ARTICLE INFO

Article history:
Received 20 December 2016
Accepted 27 January 2017
Available online 10 February 2017

Keywords:
Nucleation
Glass transition
Random anisotropy
Coercivity
Grain size

ABSTRACT

The structural and magnetic properties of amorphous $Fe_{87-y}B_{13}Cu_y$ ($y = 0$ to 1.5) annealed with a range of heating rates (α) up to 150 K/s were investigated. The lowest coercivity (H_c) for $Fe_{87}B_{13}$ after crystallization shows a dramatic decrease from 174 A/m to 6.7 A/m when α is increased from 1.7 K/s to 150 K/s. The coercivity of $Fe_{87-y}B_{13}Cu_y$ annealed at 150 K/s is reduced by Cu addition and $H_c = 3.0$ A/m is obtained at $y = 1.5$. Nanostructures with a grain size of 15 to 20 nm were evident in transmission electron micrographs from these rapidly annealed alloys.

1. Introduction

Crystallization of Fe-based amorphous precursors has been known to be an effective processing route for preparing magnetically soft microstructures [1–7] where bcc-Fe nanocrystallites are embedded in an amorphous matrix [8]. The magnetic softness in these nanocrystalline materials is due to the exchange-softening effect [9,10] under a condition where the grain size is smaller than the exchange correlation length. An advantage of such Fe-based nanocrystalline alloys is that the reduction of the intrinsic magnetocrystalline anisotropy (K_1) is no longer an essential requirement for the magnetic softness. Hence, the content of nonmagnetic additives can be lower in nanocrystalline soft magnetic materials as compared with those of the conventional crystalline alloys. This potentially leads to a higher saturation magnetization (M_s) in the nanocrystalline alloys. Still, the vast majority of nanocrystalline soft magnetic alloys developed to date contain a considerable amount of nonmagnetic elements because additives such as P [7], Nb [1,2] and/or Cu [1,2,4–7] are needed for the formation of homogeneous nanostructures and thus, their highest saturation magnetization remains approximately 1.85 T [6,11].

It is known [12] that the technical magnetic properties of soft [13,14] and hard [15–17] magnetic materials prepared from precursor amorphous alloys often depend on the heating rate during annealing processes. It has been demonstrated for an amorphous $Fe_{90}Zr_7B_3$ alloy that the average grain size after primary crystallization decreases from 19.3 nm to 13.3 nm by increasing heating rate from 0.042 K/s to 3.3 K/s [13]. As a result, the initial permeability of this nanocrystalline alloy at 1 kHz was enhanced by 10-fold to 22,000. Recently, a high heating rate above 100 K/s was realized by using a pair of preheated Cu blocks for annealing [18,19]. This rapid heating technique opens the possibility for significant reductions of nonmagnetic additives in Fe-based nanocrystalline soft magnetic alloys because the grain refinement is promoted by the heating process. In this study, to explore the potential of rapid annealing in nanocrystalline soft magnetic materials, we have investigated the effect of heating rate during primary crystallization on the structural and soft magnetic properties of Fe-B based melt-spun alloys.

2. Experimental procedures

Ingots of $Fe_{100-x-y}B_xCu_y$ ($x = 13$ to 17; $y = 0$ to 1.5) were prepared by an Ar-arc melting furnace. Amorphous ribbons with a thickness of approximately 15 μm were prepared from these ingots by single-roller melt spinning in an Ar atmosphere. The melt-spun ribbons were annealed both conventionally at 1.7 K/s by using an infrared furnace under a reduced pressure ($<10^{-2}$ Pa) and also rapidly using a pair of preheated Cu blocks under a N_2 atmosphere. The heating rate in the latter method was moderated between 3 and 150 K/s by adding thin alumina fiber sheets between the sample and the block. As-cast and annealed structures were examined by x-ray diffraction (XRD) and transmission electron microscopy (TEM); a FEI Tecnai-T20 TEM

* Corresponding author.
E-mail address: Kiyonori.suzuki@monash.edu (K. Suzuki).

http://dx.doi.org/10.1016/j.scriptamat.2017.01.030
1359-6462/

operated at 200 kV was used. XRD patterns were also used for estimating the average grain size; the instrumental broadening effect on the goniometer was corrected by using a pure-Fe sample annealed at 1273 K for 28.8 ks. Differential thermal analysis (DTA) was carried out at a constant heating rate of 0.67 K/s. The saturation magnetization (M_s) and coercivity (H_c) were measured by a vibrating-sample magnetometer (VSM) and a dc *B-H* tracer.

3. Results and discussion

Fig. 1(a) shows the bright-field electron micrograph and the corresponding selected area diffraction pattern for the melt-spun $Fe_{87}B_{13}$ alloy. The microstructure is free of crystallites and the diffraction pattern exhibits a halo pattern, confirming the formation of an amorphous phase by melt-spinning. In our experiment, 13 at.% was the minimum B content for obtaining fully amorphized melt-spun ribbons. In Fig. 1(b) we show the DTA curves for amorphous $Fe_{100-x}B_x$ ($x = 13$ to 17) alloys. Two exothermic peaks are seen on all the DTA curves except $x = 17$. The crystallization behaviours of amorphous Fe-B alloys have been studied extensively [20,21] and the first exothermic reaction of this two-step process is a well-known example of primary crystallization where bcc-Fe crystallites start to precipitate in an amorphous matrix. The second exothermic peak arises from the decomposition of this residual amorphous matrix and Fe_3B and/or Fe_2B compounds form during this second-stage reaction. The onset temperature of primary crystallization shows a tendency to increase with B content while the trend is opposite for the secondary crystallization reaction. As a result, the onsets of the two reactions meet for $x = 17$ and the crystallization process becomes single-step, resulting in the formation of bcc-Fe and Fe_3B concurrently upon crystallization. Hence, the largest temperature interval between the two reactions is seen for $x = 13$ in the $Fe_{100-x}B_x$ alloys. In Fig. 1(b) the DTA curve obtained from amorphous $Fe_{85.5}B_{13}Cu_{1.5}$ is also shown. The onset temperatures of primary crystallization for this alloy is lower than that of the Cu-free $Fe_{87}B_{13}$ alloy, resulting in a larger temperature interval between the two exothermic reactions. This effect of Cu addition is readily understood by the well-known Cu cluster formation [8,22] with which the kinetics of heterogeneous nucleation is accelerated significantly upon primary crystallization.

Fig. 2 shows the change in the coercivity (H_c) as a function of annealing temperature (T_a) for amorphous $Fe_{87}B_{13}$ and $Fe_{85.5}B_{13}Cu_{1.5}$. These two alloys are chosen primarily because they exhibit large temperature intervals between the primary and secondary crystallization reactions. A large temperature interval between the two crystallization reactions is ideal for the formation of a magnetically-soft microstructure where bcc-Fe grains are embedded in a residual amorphous phase. Both the amorphous alloys were annealed conventionally with a constant

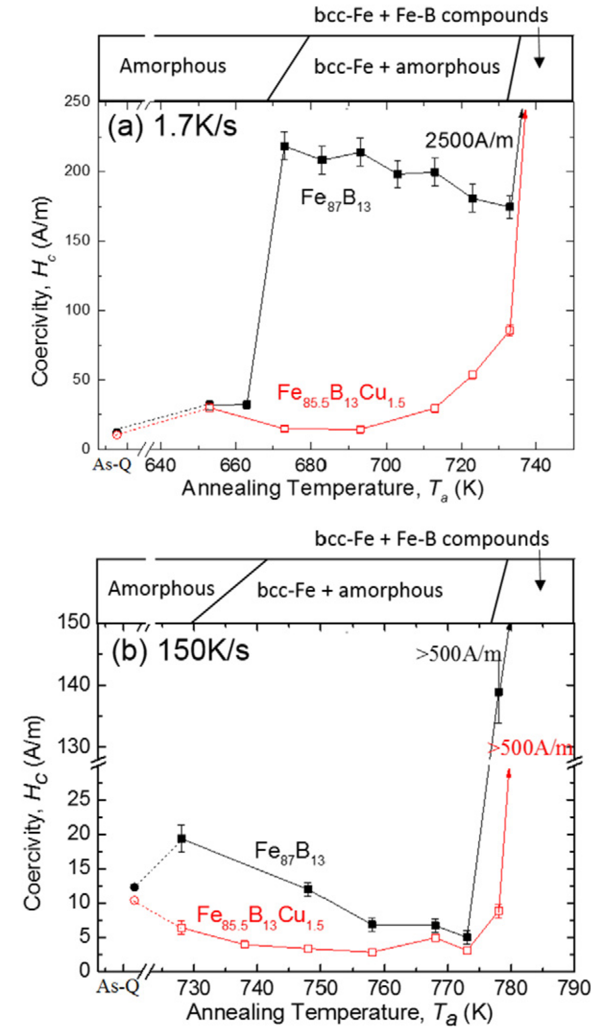

Fig. 2. Change in coercivity (H_c) as a function of annealing temperature (T_a) for $Fe_{87}B_{13}$ and $Fe_{85.5}B_{13}Cu_{1.5}$ with a heating rate of (a) 1.7 K/s and (b) 150 K/s.

heating rate of 1.7 K/s and also rapidly by a pair of preheated Cu blocks under a N_2 atmosphere. The average heating rate of the latter is 150 K/s between 670 K and 710 K where primary crystallization starts to takes place. The annealing time for the conventional and rapid annealing was 300 s and 3 s, respectively. The results of structural characterization on annealed samples by means of X-ray diffraction and TEM are also

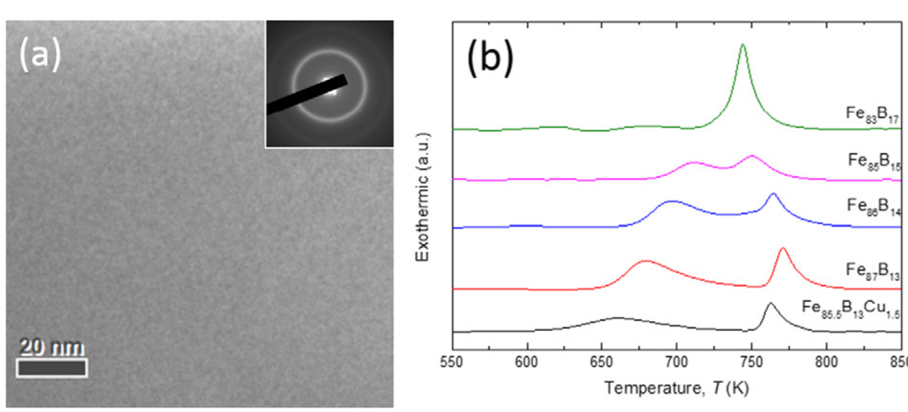

Fig. 1. (a) Bright-field transmission electron micrograph and selected area diffraction pattern for melt-spun $Fe_{87}B_{13}$ and (b) differential thermal analysis curves for amorphous $Fe_{100-x}B_x$ ($x = 13$ to 17) and $Fe_{85.5}B_{13}Cu_{1.5}$.